

NO-A184 994

MAGNETOCALORIC REFRIGERATION(U) DAVID M TAYLOR NAVAL
SHIP RESEARCH AND DEVELOPMENT CENTER BETHESDA MD
G GREEN ET AL. MAR 87 DTNSRDC-87/032

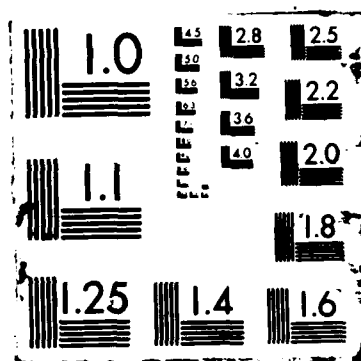
1/1

UNCLASSIFIED

F/G 13/1

ML

END
H E
D H



FILE COPY

(12)

AD-A184 994

David W. Taylor Naval Ship Research and Development Center
Bethesda, MD 20084-5000

DTNSRDC-87/032 March 1987

Propulsion and Auxiliary Systems Department
Research and Development

Magnetocaloric Refrigeration

by

Geoffrey Green, George Patton,
John Stevens, James Humphrey

DTIC
ELECTE
SEP 18 1987
S D

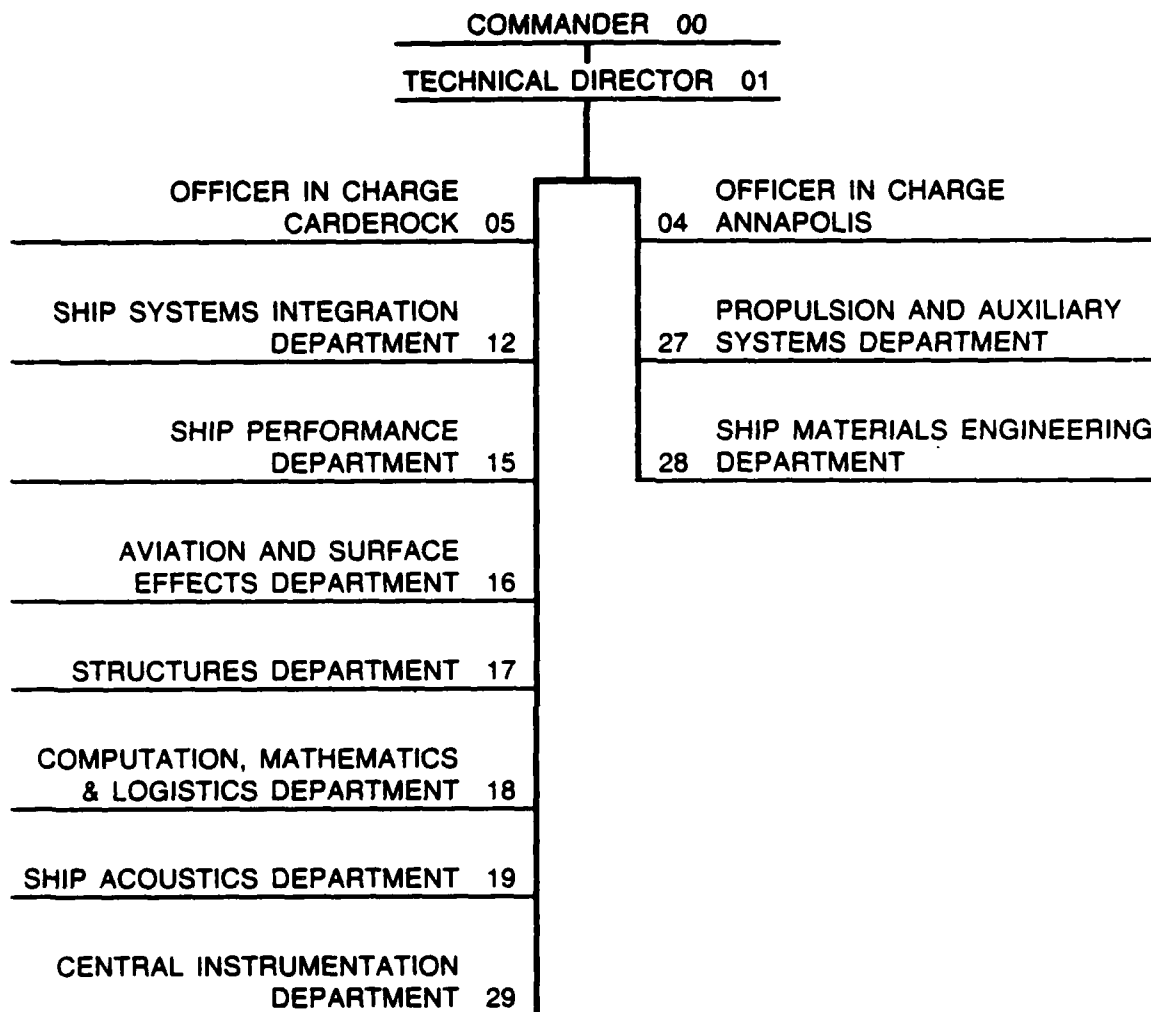
DTNSRDC/87/032 Magnetocaloric Refrigeration



Approved for public release; distribution is unlimited.

87 9 18 090

MAJOR DTNSRDC TECHNICAL COMPONENTS



UNCLASSIFIED

SECURITY CLASSIFICATION OF THIS PAGE

ADA184994

REPORT DOCUMENTATION PAGE

1a REPORT SECURITY CLASSIFICATION UNCLASSIFIED			1b RESTRICTIVE MARKINGS	
2a SECURITY CLASSIFICATION AUTHORITY			3 DISTRIBUTION/AVAILABILITY OF REPORT Approved for public release; distribution is unlimited.	
2b DECLASSIFICATION/DOWNGRADING SCHEDULE				
4 PERFORMING ORGANIZATION REPORT NUMBER(S) DTNSRDC/87/032			5 MONITORING ORGANIZATION REPORT NUMBER(S)	
6a NAME OF PERFORMING ORGANIZATION David Taylor Naval Ship R&D Center		6b OFFICE SYMBOL (if applicable)	7a NAME OF MONITORING ORGANIZATION	
6c ADDRESS (City, State, and ZIP Code) David Taylor Naval Ship R&D Center Bethesda, MD 20084-5000			7b ADDRESS (City, State, and ZIP Code)	
8a NAME OF FUNDING/SPONSORING ORGANIZATION DTNSRDC/IRIED		8b OFFICE SYMBOL (if applicable) Code 012	9 PROCUREMENT INSTRUMENT IDENTIFICATION NUMBER	
8c ADDRESS (City, State, and ZIP Code) Bethesda, MD 20084-5000			10 SOURCE OF FUNDING NUMBERS	
			PROGRAM ELEMENT NO 62766N	PROJECT NO
			TASK NO RZ66-300	WORK UNIT ACCESSION NO 2712-150
11 TITLE (Include Security Classification) Magnetocaloric Refrigeration				
12 PERSONAL AUTHOR(S) Green, G., G. Patton, J. Stevens and J. Humphrey				
13a TYPE OF REPORT Research & Development		13b TIME COVERED FROM TO	14 DATE OF REPORT (Year, Month, Day) March 1987	
15 PAGE COUNT 43				
16 SUPPLEMENTARY NOTATION				
17 COSATI CODES			18 SUBJECT TERMS (Continue on reverse if necessary and identify by block number)	
FIELD	GROUP	SUB-GROUP	Magnetocaloric refrigerator	
			Gadolinium	
			Curie temperature	
19 ABSTRACT (Continue on reverse if necessary and identify by block number)				
<p>The magnetocaloric refrigerator uses the adiabatic temperature response of ferro-magnetic materials (rare-earth metals) in a high magnetic field. A mathematical model of a reciprocating magnetic refrigerator having an active element of a rare-earth metal predicted that a 60-K temperature span could be achieved. Based on the model's results, an experimental refrigerator was fabricated and the thermal characteristics of an active regenerator in a reciprocating apparatus were measured. The active material was gadolinium which has a Curie temperature of 293 K and was formed into an embossed ribbon geometry. Significant regeneration in the magnetic material was observed, and a 50-K temperature span was achieved. A cold end temperature of 246 K was measured.</p> <p>The results indicated that the active regeneration concept can successfully produce magnetocaloric refrigeration at temperatures near the Curie temperature of the material,</p> <p style="text-align: right;">(continued on reverse side)</p>				
20 DISTRIBUTION AVAILABILITY OF ABSTRACT <input checked="" type="checkbox"/> UNCLASSIFIED UNLIMITED <input type="checkbox"/> SAME AS RPT <input type="checkbox"/> DTIC USERS			21 ABSTRACT SECURITY CLASSIFICATION Unclassified	
22a NAME OF RESPONSIBLE INDIVIDUAL Geoffrey Green			22b TELEPHONE (Include Area Code) 301-267-3632	22c OFFICE SYMBOL 2712

UNCLASSIFIED

SECURITY CLASSIFICATION OF THIS PAGE

Block 19

and the measured temperature span verified the mathematical model developed to describe the process.

Further, if the active magnetic element were a combination of several rare-earth metals having significant magnetocaloric effects at decreasing temperatures, the possibility exists for producing a single-stage magnetic refrigerator that could operate over a very large temperature span. ←

Accession For	
NTIS CRA&I	<input checked="" type="checkbox"/>
DTIC TAB	<input type="checkbox"/>
Unannounced	<input type="checkbox"/>
Justification	
By	
Distribution /	
Availability Codes	
Dist	Avail and/or Special
A-1	



UNCLASSIFIED

CONTENTS

	Page
NOTATION.....	v
ABSTRACT.....	1
ADMINISTRATIVE INFORMATION.....	1
INTRODUCTION.....	1
BASIC PRINCIPLES OF MAGNETIC REFRIGERATION.....	3
MODELING THE MAGNETOCALORIC EFFECT.....	8
THE CONCEPT.....	9
THE MATHEMATICAL MODEL.....	10
EXPERIMENTAL VERIFICATION OF THE MODEL.....	18
RESULTS.....	26
ACKNOWLEDGEMENT.....	30
APPENDIX - CLASSICAL MOLECULAR FIELD THEORY.....	31

FIGURES

1. Entropy-temperature characteristic for a magnetocaloric effect.....	5
2. Adiabatic temperature change vs. temperature for a ferromagnetic material having a magnetocaloric effect.....	6
3. Thermodynamic refrigeration; Carnot and Brayton cycles.....	7
4. Magnetic refrigeration concept.....	9
5. Magnetocaloric characteristics of gadolinium.....	11
6. Magnetic field distribution with and without the gadolinium active regenerator in the bore of the magnet.....	12
7. Calculated magnetic refrigeration cooling characteristics.....	15
8. Magnetocaloric characteristics of three rare-earth metals.....	16

	Page
9. Calculated final temperature distribution of the three-element combination active ferromagnetic regenerator.....	17
10. Superconducting magnet used in the experimental magnetic refrigerator.....	19
11. Magnetic field distribution along the axis of the superconducting magnet.....	20
12. Magnetic refrigerator apparatus.....	21
13. Gadolinium ribbon regenerator section in the G-10 fiberglass sleeve.....	21
14. Finned tube heat exchanger.....	22
15. Magnetic refrigerator assembly.....	24
16. Calculated mass flow characteristics based on a linear approximation of the adiabatic magnetization process.....	25
17. Measured adiabatic magnetization characteristics for Gd ribbon.....	27
18. Measured cool-down profile of the magnetic refrigerator.....	28
19. Measured temperature distribution of the Gd active magnetic regenerator.....	29

NOTATION

Ag	Surface area of the gadolinium, cm^2
Af	Contact area of the fluid, cm^2
Am	Area of the surface between the material and fluid, cm^2
As	Surface area of the stainless steel, cm^2
B	Magnetic field, Tesla (T)
C _b	Heat capacity at constant field, J/mole-K (Joules per mole-Kelvin)
C _f	Heat capacity of the fluid, $\text{cal}/\text{cm}^3\text{-K}$
C _m	Heat capacity of material, $\text{cal}/\text{cm}^3\text{-K}$
C _p	Specific heat of the fluid, $\text{cal}/\text{g-K}$
h	Convection coefficient, $\text{cal}/\text{s cm}^2\text{-K}$
k _f	Thermal conductivity of the fluid, $\text{cal}/\text{s-cm-K}$
k _m	Thermal conductivity of material, $\text{cal}/\text{s-cm-K}$
M	Magnetization, A^2/mole
P	Pressure, atm
S	Entropy, J/mole-K
T	Temperature, K
t	Time, s
T _f	Temperature of fluid, K
T _g	Temperature of material, K
T _m	Temperature of material, K
T _s	Temperature of stainless steel, K
V	Velocity of the fluid, cm/s
V _f	Volume of fluid, cm^3
V _m	Volume of material, cm^3

x Axial length, cm

ρ_m Density of material, g/cm³

ρ_f Density of fluid, g/cm³

ABSTRACT

The magnetocaloric refrigerator uses the adiabatic temperature response of ferromagnetic materials (rare-earth metals) to a high magnetic field as a basis for operation. A mathematical model of a reciprocating magnetic refrigerator having an active element of a rare-earth metal predicted that a 60-K temperature span could be achieved. Based on the model's results, an experimental refrigerator was fabricated and the thermal characteristics of an active regenerator in a reciprocating apparatus were measured. The active material was gadolinium, which has a Curie temperature of 293 K and was formed into an embossed ribbon geometry. Significant regeneration in the magnetic material was observed, and a 50-K temperature span was received. A cold end temperature of 246 K was measured.

The results indicated that the active regeneration concept can successfully produce magnetocaloric refrigeration at temperatures near the Curie temperature of the material, and the measured temperature span verified the mathematical model developed to describe the process.

Further, if the active magnetic element were a combination of several rare-earth metals having significant magnetocaloric effects at decreasing temperatures, the possibility exists for producing a single-stage magnetic refrigerator that could operate over a very large temperature span.

ADMINISTRATIVE INFORMATION

This work was performed under the David Taylor Naval Ship Research and Development Center's IR/IED project entitled, "Magnetocaloric Cryogenic Refrigeration," Work Unit 2712-150, Program Element 61152N, and Task Area ZR0240101.

INTRODUCTION

The Navy at the David Taylor Naval Ship Research and Development Center (DTNSRDC) has in the past twelve years been developing the necessary machinery for use with advanced electric propulsion systems for future ships. This equipment uses the advanced technology of superconductivity to improve the power density of large electric propulsion motors. Superconductivity occurs when certain materials are cooled

to very low temperatures (typically 5 to 20 K) and electrical resistance drops to zero. This phenomenon has been demonstrated to be very valuable for building highly efficient, high power density electrical machinery. Superconducting motors and generators require a cryogenic refrigerator to maintain the superconductor at these low temperatures. Cryogenic refrigerators have been used extensively in the laboratory where efficiency and reliability are of secondary importance. For naval shipboard applications the unit must be efficient, rugged, and reliable to meet the Navy's operational requirements. Areas of concern associated with these refrigeration systems are the compressor inefficiency, oil contamination, and engine valves and seals in the liquifier. Thus, having a shipboard liquifier that required no compressors would be highly desirable, not only to eliminate the inefficiency of the compressors but to improve the operating conditions to which the refrigerant is exposed. The compact and rugged construction of a magnetic refrigerator would also allow for operating under high shock and vibration loading such as that encountered in a Navy shipboard environment.

Until recently, the magnetic refrigerator had been used only at temperatures below 4 K. But the concept of magnetic refrigeration has shown some real possibility at temperatures greater than 4 K with the use of ferromagnetic material. The magnetic refrigerator uses the magnetocaloric effect, which allows certain materials to undergo a large adiabatic temperature change or isothermal entropy change when subjected to a large magnetic field. Using this effect, it has been proposed that a refrigerator could be designed to have a Carnot efficiency of about 50 to 70% [Barclay, 1]. In fact, Lacaze and his co-workers [2] measured efficiencies of 64% in a double-acting magnetic refrigerator at 2 K. This compares to efficiencies of about 1 to 10% for gas cycle refrigerators near liquid helium temperatures (4.2 K) as reported by Strobridge [3].

Magnetic refrigerators can be classified into four categories: (1) continuous flow (rotary); (2) periodic flow (reciprocating); (3) nonregenerative (small ΔT); and (4) regenerative (large ΔT). The rotary concept (continuous flow) is being investigated by Barclay [4] at Los Alamos National Laboratory. Dr. Barclay's work is in the 4 to 20 K temperature range with no regeneration. The reciprocating concept was investigated by Brown [5] at the National Aeronautics and Space Administration's Lewis Laboratory. He used a regeneration system in the fluid to demonstrate a large (80-K) temperature span. This work was performed near room temperature to make use of fluids with high heat capacities. A second method to obtain regeneration is to do it in the active ferromagnetic or paramagnetic material, a method described as an active regenerator in a patent application by Barclay [6].

Because the magnetic refrigeration process is reversible, the thermal and magnetic characteristics of the materials used will determine how well the concept works and thus determine the efficiency of the cycle. The key to the process is thorough understanding of the thermal and magnetic interactions, so as to keep entropy generation to a minimum. At DTNSRDC, we decided to confine the thermal and magnetic interactions to one location by use of an active regenerator in a reciprocating configuration. A mathematical model of such a system was formulated, a prototype system was built and tested, and results of the model were compared with experimental measurements.

BASIC PRINCIPLES OF MAGNETIC REFRIGERATION

The magnetic refrigerator or magnetic heat pump uses the magnetocaloric effect of a solid material to extract heat from a low-temperature source and transfer it to a higher temperature sink. The entropy change governing this process is a function of temperature (T) and magnetization (M). The total derivative of the entropy in a magnetic material is given by Eq. 1.

$$dS = \frac{\partial S}{\partial T_M} dT + \frac{\partial S}{\partial M_T} dM \quad (1)$$

Substituting some generalized thermodynamic relationships [Wark, 7] into Eq. 1 results in the following:

$$dS = \frac{C_b}{T} dT + \frac{\partial M}{\partial T_B} dB \quad (2)$$

where S is entropy, B is magnetic field, C_b is heat capacity at constant magnetic field, M is magnetization, and T is the absolute temperature. Equation 2 can be solved if the magnetic field-dependent heat capacity and the equation of state for the ferromagnetic material are known. The equation of state for a ferromagnetic material can be calculated by using the molecular-field approximation [2]. The field dependent heat capacity, on the other hand, is a quantity that must be measured because of the complex crystalline structures of the ferromagnetic material.

For an isothermal entropy change, Eq. 2 reduces to the following form:

$$dS = (\partial M / \partial T)_B dB \quad (3)$$

and for a reversible adiabatic temperature change, Eq. 2 reduces to Eq. 4.

$$dT = - \frac{T}{C_b} \frac{\partial M}{\partial T_B} dB \quad (4)$$

In addition, a paramagnetic solid that follows Curie's law will result in $(\partial M / \partial T)_B$ being negative, and thus one can make some qualitative observations. Equation 3 indicates that as the field is changed, an inverse isothermal entropy change occurs. This experimental characteristic is illustrated in Fig. 1 for a

typical ferromagnetic material. Also, Eq. 4 indicates that as the field is changed, a direct adiabatic temperature change occurs, that is, an increase in field increases the temperature, while a decrease in field decreases temperature. This phenomenon, which is illustrated in Fig. 2 for a typical ferromagnetic material, is known as the magnetocaloric effect. It is the principle upon which the development of a magnetic refrigerator is based.

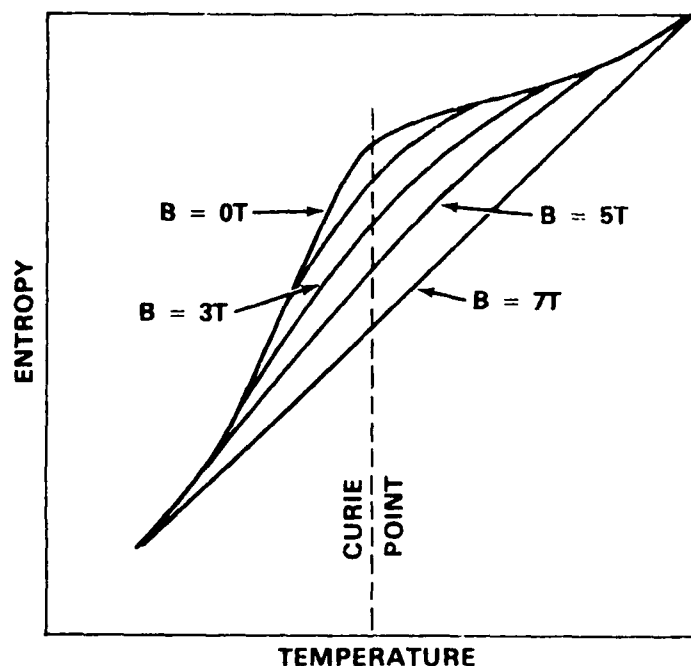


Fig. 1. Entropy-temperature characteristic for a magnetocaloric effect. (B is magnetic field, T is temperature).

If, then, the magnetocaloric effect is applied in a cyclic process, one can obtain magnetic cycles equivalent to the familiar thermodynamic gas cycles. The most familiar cycle and the basis for comparing all other cycles is the Carnot cycle. This cycle consists of two isentropic and two isothermal steps which result in heat being pumped from a low-temperature source to a high-temperature sink. Similarly, in a magnetic Carnot cycle, the heat is transferred from the low-temperature source into the high-temperature sink in isothermal steps. The Carnot cycle

is illustrated schematically in Fig. 3a. For the magnetic case this cycle can span only about half the adiabatic temperature change that the ferromagnetic material undergoes, which is typically only about 8°C at the material's Curie point.

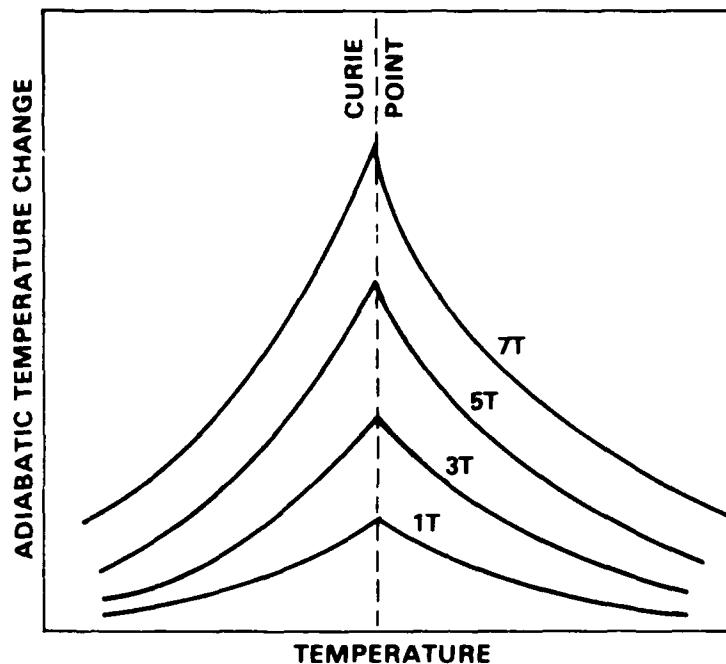


Fig. 2. Adiabatic temperature change vs. temperature for a ferromagnetic material having a magnetocaloric effect.

Larger temperature spans require a cycle with some type of heat exchange. One such cycle is the Brayton cycle. Figure 3b illustrates this cycle and compares the use to the magnetic cycle. The gas cycle process uses two isentropic steps and two isobaric steps, while the magnetic process has two isentropic steps and two isofield (constant-field) steps. The heat exchange process takes place during the isobaric steps in the gas cycle and the isofield steps in the magnetic cycle. The isentropic magnetization and demagnetization processes in the magnetic cycle are equivalent to the ideal compression and expansion processes, respectively, in the gas cycle. In a gas cycle the expansion and especially the compression stages of the cycle are not typically isentropic, but the magnetic process is isentropic.

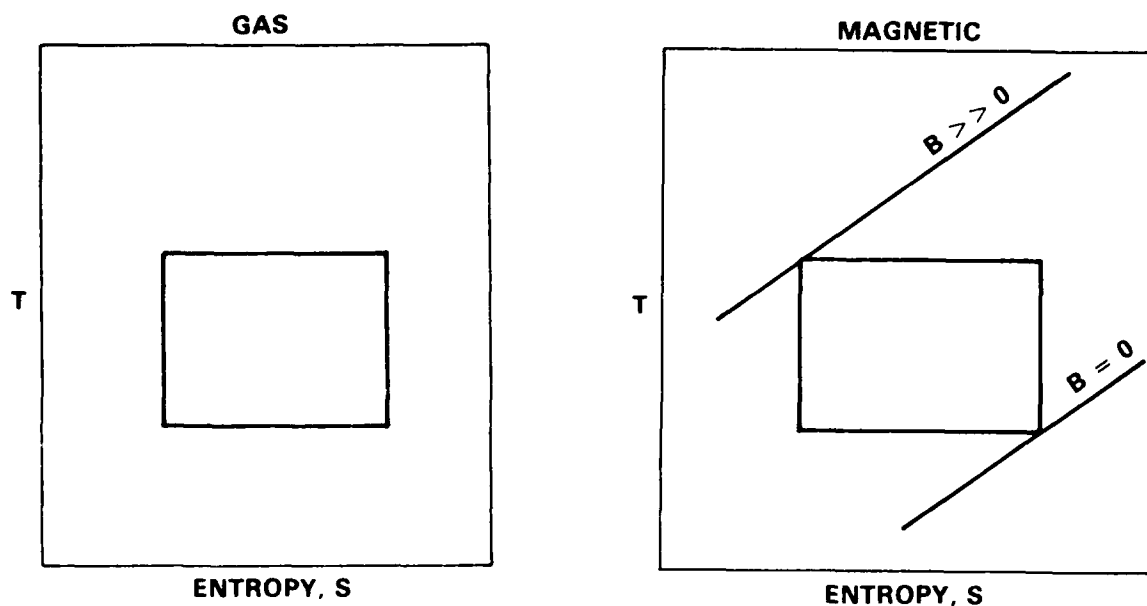


Fig. 3a. Carnot Cycle

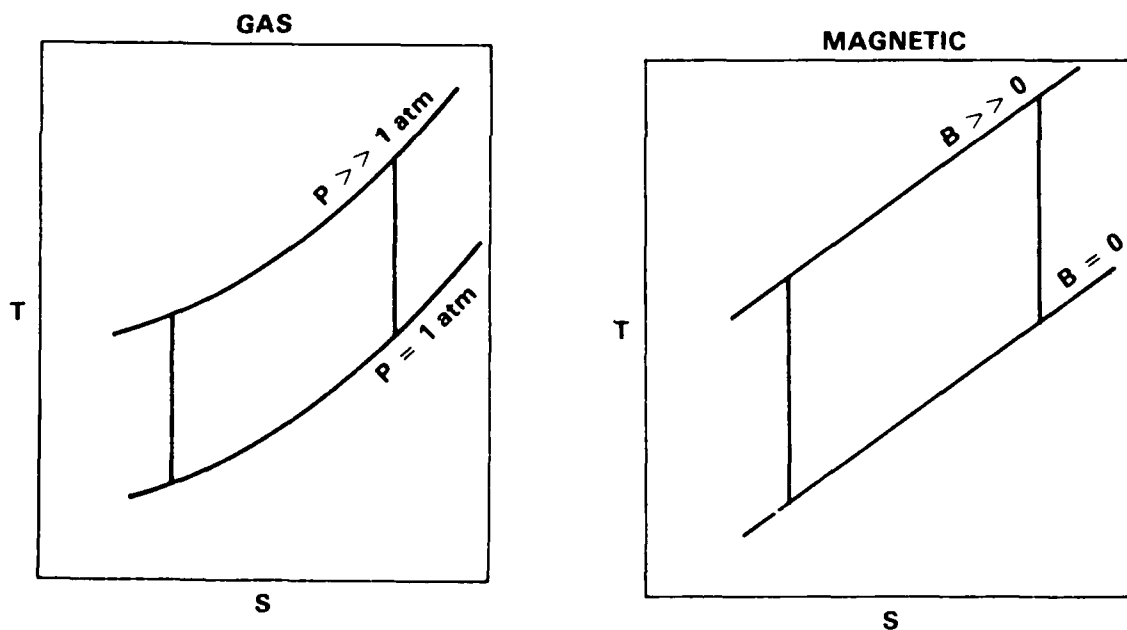


Fig. 3b. Brayton Cycle.

Fig. 3. Thermodynamic refrigeration; Carnot and Brayton cycles. (T = temperature, S = entropy, B = magnetic field, and P = pressure).

The isentropic nature of the process is the basis for the much higher efficiency possible in magnetic refrigeration. In fact, the power required for a magnetic cycle has been estimated to be 50-70% of Carnot, as compared with 5 to 10% of Carnot for a gas cycle. Thus a great efficiency advantage exists for a magnetic refrigerator if efficient heat transfer is obtainable.

In any cycle comparison, the magnitude of the refrigeration cooling that takes place in each cycle is also important. The isentropic temperature change for a typical magnetic refrigerator is only 16°C, while a gas cycle refrigerator expanding gas from 15 to 1 atmosphere near room temperature can result in an isentropic temperature change of about 150°C. The refrigeration capacity of these two cycles is best compared by using the isothermal entropy change. In a comparison based on a unit of mass, the gas cycle is better than the magnetic cycle by a factor of 20 near room temperature, but the advantage decreases with decreasing temperature.

If the two cycles are compared based on the volume they require, the magnetic refrigerator at room temperature is better by a factor of 50, because the density of a ferromagnetic solid is 1000 times greater than the density of a gas at standard conditions. The conclusion would be that ideally the magnetic refrigerator is a more compact process. However, this compactness presents the problem that the heat exchanger must operate in a much smaller volume. In a small volume, the required high heat exchanger effectiveness is much more difficult to obtain.

MODELING THE MAGNETOCALORIC EFFECT

The magnetic refrigeration process utilizing the magnetocaloric effect on a ferromagnetic material was investigated. The primary focus of the study was to obtain an understanding of heat transfer and more specifically the regeneration process in a magnetic Brayton cycle.

THE CONCEPT

The experimental apparatus used to study a regenerator in a magnetic refrigerator is shown schematically in Fig. 4. The magnetic refrigerator consisted of five major parts: (1) the high field system, consisting of a superconducting magnet surrounded by a pool of liquid helium and contained in a vacuum-insulated Dewar flask; (2) the ferromagnetic material, gadolinium, a rare-earth metal having a Curie point of 293 K; (3) the displacer, which moves the fluid through the ferromagnetic material to perform the heat exchange; (4) the warm heat exchanger, which removes the heat produced in the adiabatic magnetization process; and (5) the copper regenerator, which isolates the cold section of the refrigerator from the warm mixing chamber of the displacer.

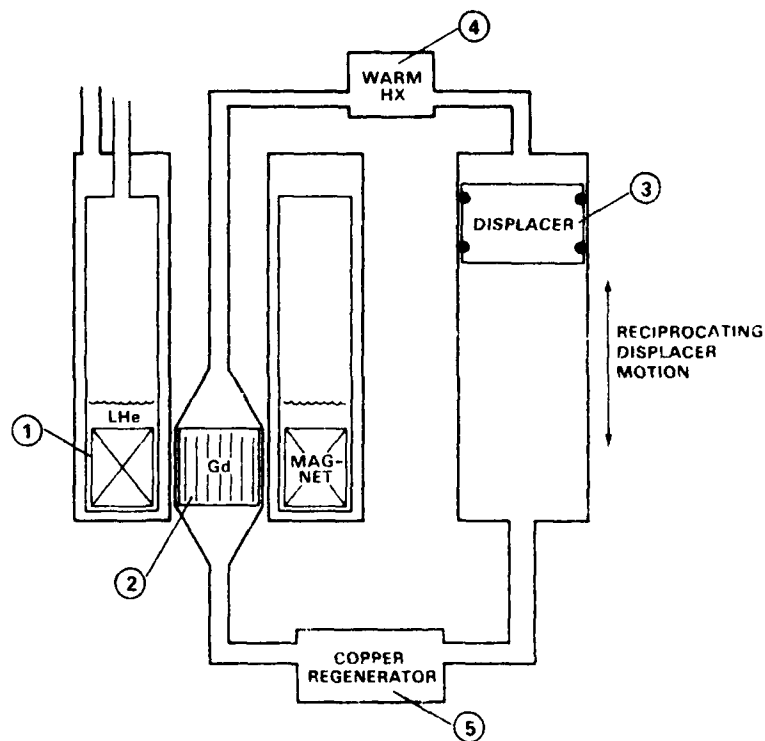


Fig. 4. Magnetic refrigeration concept.

The configuration used for the active magnetic material in the model was strips of embossed gadolinium ribbon wound into nearly flat, circular sections (called "pancakes") and then stacked together so as to fill a fiberglass sleeve. This configuration allowed maximum contact area between the magnetic material and the working fluid, and could in fact be fabricated when the model was verified experimentally (see also Green et al.) [8].

In the model, the magnetic cycle takes place as follows: (1) The magnet is ramped up to full field, causing the ferromagnetic material to heat up. (This step is equivalent to the compression process in a gas cycle.) (2) The displacer moves down, pushing the working fluid, nitrogen, through the ferromagnetic material and removing the heat of the magnetization process. This heat is carried to the warm heat exchanger and carried off by the counterflowing water circuit. (3) The magnetic field is removed, cooling the gadolinium through an adiabatic demagnetization process. (4) The displacer is moved up, and the fluid is cooled as it passes through the ferromagnetic material cooling the volume between the cold end of the gadolinium and the copper regenerator.

THE MATHEMATICAL MODEL

The ferromagnetic material, gadolinium, can produce a significant adiabatic temperature change when subjected to a high magnetic field. An adiabatic temperature change of 14°C was measured by Benford and Brown [9] near its Curie temperature under a 7-T field (Fig. 5). The magnetic refrigerator is based on this adiabatic temperature change and the thermal exchange mechanism of the regeneration process, which also occurs in the ferromagnetic, or "active," material.

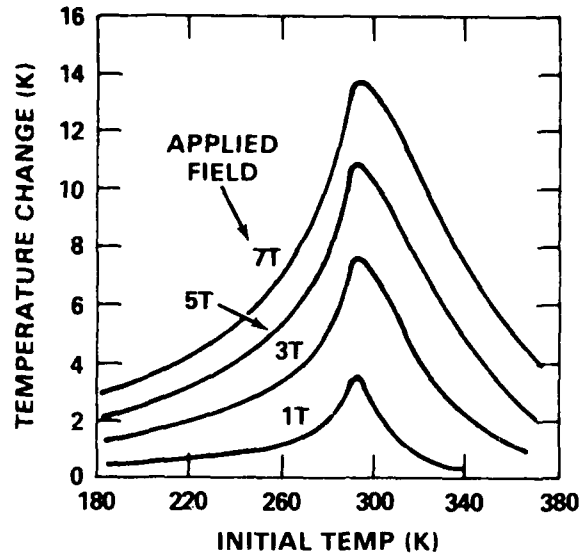


Fig. 5. Magnetocaloric characteristics of gadolinium.

To help us better understand this process, we formulated a numerical model of the magnetic field and thermal interactions. The magnetic refrigerator involves four steps per cycle to obtain the cooling effect in a cyclic process. They are:

- Magnetize the material
- Remove the heat of magnetization
- Demagnetize the material
- Cool the load

The magnetic refrigeration cycle is a continuous thermal transient process. One could visualize this transient process as a thermal wave that passes through the active material every half cycle. The heat of magnetization is removed and the load cooled by a pressurized gas passed through the magnetic material periodically every half cycle.

A 2-dimensional triangular irregular mesh computer program (called TRIM) [10] was used to calculate the magnetic field produced by the superconducting magnet indicated in Fig. 4.

Initial calculations assumed no ferromagnetic material in the bore of the magnet. This configuration was impractical, however, because the ferromagnetic material (gadolinium) had certain magnetic properties. The permeability of gadolinium was calculated based on the classical molecular field theory described in the appendix. The permeability of the gadolinium as a function of field was then used in the TRIM program to calculate the magnetic field in the gadolinium. To simulate the geometry of the gadolinium a series of 0.0635-cm-thick concentric rings spaced 0.0635 cm apart were modeled. The field distribution with and without and concentric gadolinium rings in the bore of the magnet is illustrated in Fig. 6.

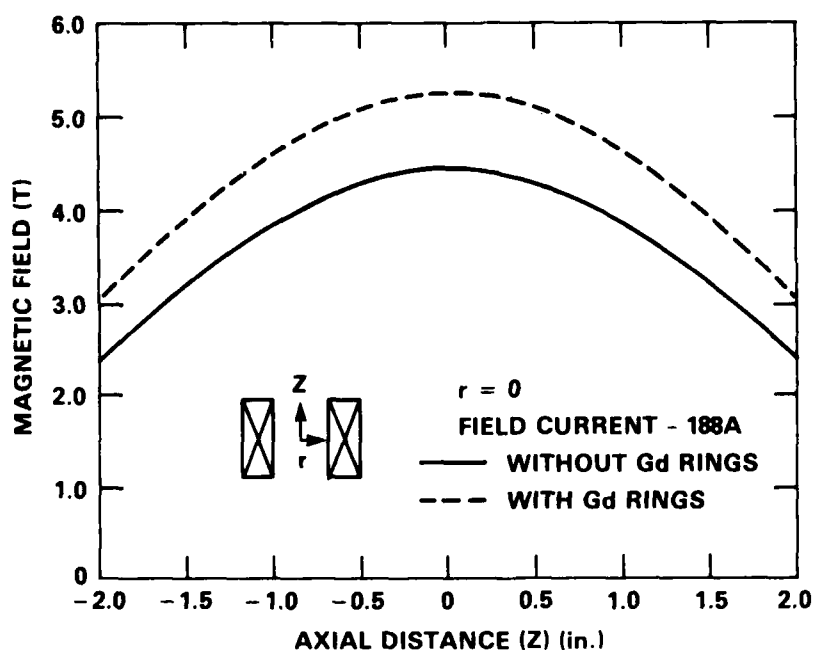


Fig. 6. Magnetic field distribution with and without the gadolinium active regenerator in the bore of the magnet.

These results indicated that the axial field in the gadolinium rings was about 18% higher than without the gadolinium. The magnetic analysis also showed that a drop in magnetic field of 73% occurred between the center and the end of the gadolinium. The unexpectedly large nonuniform field distribution was sure to have a drastic

effect on the thermal performance of a magnetic refrigerator, and it was minimized in the experimental apparatus by use of a magnet that was long in relation to the gadolinium element.

The magnetic refrigerator performance, in which the gadolinium undergoes the adiabatic temperature change and performs the regeneration, was modeled using a finite element program NASTRAN [11]. In our study only the gadolinium, the cyclic fluid motion, and the stainless steel container were modeled. The model was considered to have a uniform radial temperature gradient and thus a 1-dimensional thermal geometry. We also assumed that the temperature entering the gadolinium from the warm end was constant (room temperature) and that the temperature entering the gadolinium from the cold end was the weighted average of the initial and final temperature of the gas exiting from the gadolinium during previous half cycle. The other boundary conditions were assumed to be adiabatic. The partial differential equation for the gadolinium and the stainless steel cylinder is as follows:

$$\rho_m = C_m \frac{\partial T_m}{\partial t} - k_m \nabla^2 T_m = \frac{A_m h}{V_m} T_f - T_m \quad (5)$$

and the partial differential equation for the fluid is given by Eq. 6:

$$\rho_f C_f \frac{\partial T_f}{\partial t} - k_f \nabla^2 T_f = - \rho_f C_p V \frac{\partial T_f}{\partial x} + \frac{A_g h}{V_f} T_g - T_f + \frac{A_f h}{V_f} T_s - T_f \quad (6)$$

In addition, the following assumptions were made:

- The magnetic field in the gadolinium calculated with TRIM is correct.
- The heat capacity of gadolinium as a function of temperature calculated by Griffel et al. [12] is correct.

- Thermal conductivity in gadolinium is not a function of temperature.
- The adiabatic demagnetization temperature change as measured by Benford and Brown [9] is accurate.
- The working fluid obeys the ideal gas law.
- The heat transfer coefficient determined using the gap regenerator data from Kays and London [13] is accurate.
- The contact area between layers of gadolinium is about one-tenth of the cross sectional area.
- The ineffectiveness and heat capacity of the copper regenerator is not significant for the isothermal boundary condition.

The finite element math model consisted of eight elements for the gadolinium, eight elements for the working fluid (nitrogen gas) and eight elements for the stainless steel container. A transient thermal analysis was performed between each magnetization and demagnetization step of a cycle, assuming a uniform field of 5-T over the complete length of the gadolinium material during the magnetization step. The baseline performance was calculated based on the assumptions listed, with the results plotted in Fig. 7.

For the second scenario modeled, we assumed that the gadolinium ribbon was sliced into pancakes thinner than the original 3.8 cm, and an equivalent thermal resistance was calculated based on 0.32-cm thick pancakes having a total stack length of 15.24 cm. This configuration gave 0.07 the thermal conductance compared with the original baseline case. Although the improvement was small for this case, a larger temperature span would amplify the advantage of the reduced thermal conductance.

In the third scenario, we again assumed resistance based on the thinner gadolinium ribbon pancakes and, in addition, assumed a uniform 7-T magnetic field over the complete length of the gadolinium material. This drastically changed the refrigeration capacity and the available temperature span obtainable using gadolinium. In fact, a 60-K temperature span was calculated. This result is compared to the

previous two cases in Fig. 7. The third scenario for cold end temperature predictions calculated with this finite element model agreed closely with the measurements made by Brown [5] in his experiments using a 7-T field. These calculations indicate the significance of having a high magnetic field throughout the length of the gadolinium.

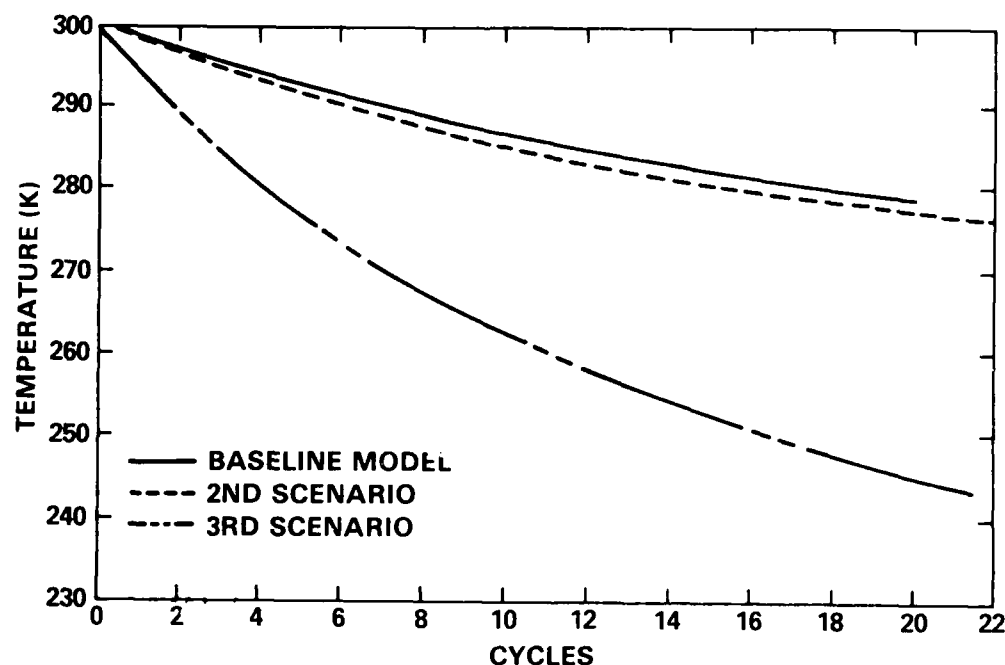


Fig. 7. Calculated magnetic refrigeration cooling characteristics. For the second scenario modeled, the Gd ribbon was sliced into thinner sections, producing a thermal conductivity 0.01 times that of the baseline model; for the third scenario, a constant magnetic field of 7T was used in addition to the thinner Gd ribbon.

To span even larger temperatures in a single stage of a magnetic refrigerator, several active magnetic elements could be stacked on top of each other in order of decreasing Curie temperature. This would result in a greater average adiabatic temperature change in the demagnetization process over a much wider temperature span. Three materials that might have these characteristics are gadolinium (Gd) [9], terbium (Tb), and dysprosium (Dy) [15]. The magnetocaloric effect for these is illustrated in Fig. 8. The characteristics shown for terbium were assumed to be similar to gadolinium and dysprosium due to terbium's similar heat capacity characteristics.

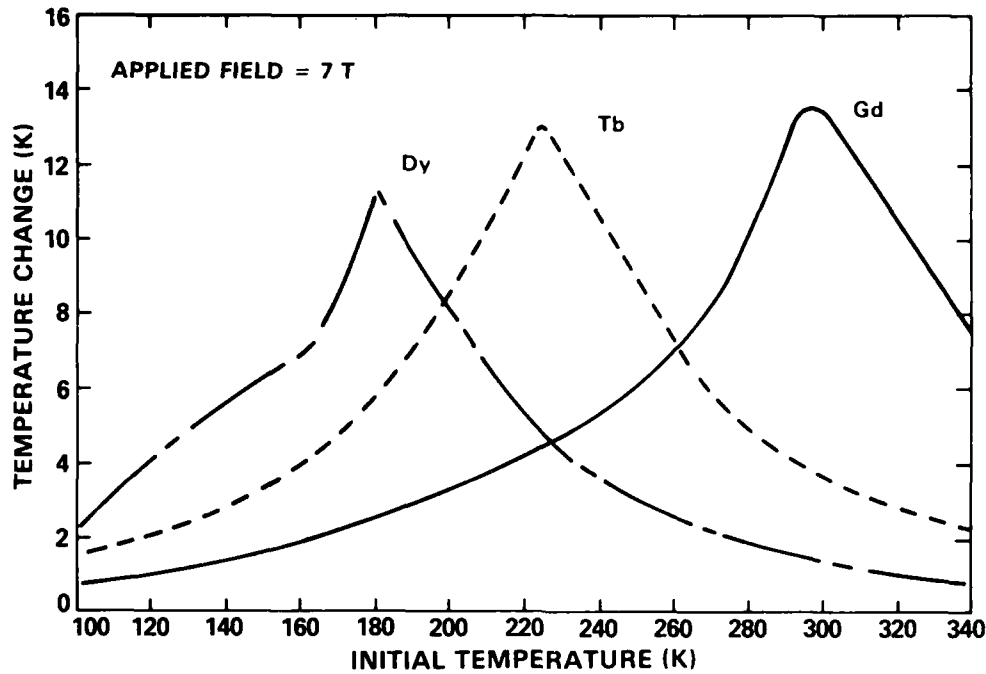


Fig. 8. Magnetocaloric characteristics of three rare-earth metals.

These three materials were assumed to have the properties shown in Fig. 8. They were entered into the finite element model as a combination of several stacked active magnetic elements and their performance calculated assuming a constant 7T magnetic field over the full length of the active magnetic elements. The most important characteristic of this particular configuration was the heat capacity of the rare-earth metals in the cool-down process. The cool-down time was greatly increased by the additional heat capacity of the rare-earth metals, which had a small magnetocaloric effect at the higher temperatures. In order to optimize the small magnetocaloric effect and minimize the heat capacities of the inactive rare-earth metals while they are being cooled to their Curie points, half the volume of

the combination active magnetic element was assumed to be filled with gadolinium, two-thirds of the remaining volume was terbium, and the rest was filled with dysprosium. The resulting prediction was that a 160-K temperature span is possible, with the lowest temperature being 140 K, as indicated in Fig. 9.

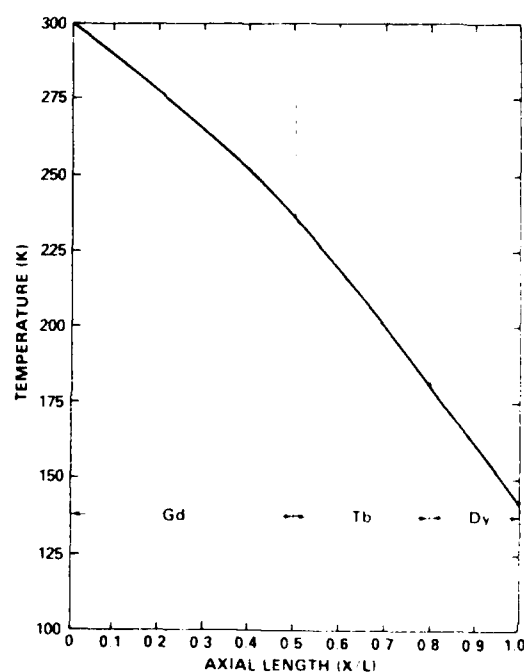


Fig. 9. Calculated final temperature distribution of the three-element combination active ferromagnetic regenerator.

The optimization of these materials is critical in both the cool-down and temperature span of the active ferromagnetic regenerator. In fact, extremely large temperature spans may be possible in a single-stage refrigerator, if the refrigerator is properly designed in relation to the thermal and magnetic characteristics of the active ferromagnetic regenerator.

EXPERIMENTAL VERIFICATION OF THE MODEL

The experimental apparatus needed to measure the thermal performance of the magnetocaloric effect in an active regenerator was designed and fabricated at DTNSRDC. This prototype refrigerator was designed to simulate a reciprocating magnetic refrigerator having a single stage, and its operation was similar to the concept shown in Fig. 4 and described above under "Modeling the Magnetocaloric Effect." The measurements obtained from experimental tests on the refrigerator were compared to results of the mathematical model discussed in the previous section.

The experimental apparatus consisted of five basic components as follows:

1. Superconducting magnet
2. Heat exchanger
3. Passive regenerator
4. Active ferromagnetic regenerator
5. Displacer

The superconducting magnet, fabricated using a niobium-titanium superconductor in a copper matrix, consisted of some 7122 turns. This magnet was designed in a solenoid configuration having a length $1\frac{2}{3}$ times that of the ferromagnetic material, assuring that the magnetic field in the ferromagnetic material would be reasonably uniform and have a magnitude of about 7 T. The magnet was 25.4 cm long. The bore diameter was 8.31 cm and the outside diameter 12.13 cm. The solenoid magnet had an inductance of 1.51 H and it could be ramped up to 225 A with a 12-V power supply in approximately 28 seconds.

Figure 10 shows the superconducting solenoid magnet attached to its support structure and the magnet connected to a pair of vapor-cooled leads. A cryogenic Dewar flask with a warm bore of 5.46 cm was constructed to hold the magnet and provide the vacuum insulation for the liquid helium. The magnet's Dewar flask had two

vapor-cooled shields at 20 and 80 K to keep the heat load to the helium at a minimum. A steady-state boil-off rate of 1 liter of liquid helium per hour was measured as the heat load conditions for the Dewar flask. Figure 11 shows the calculated and measured magnetic field distribution along the axis of the magnetic solenoid with the magnet current at 225 A. Superimposed on Fig. 11 is a representation of the active ferromagnetic regenerator (gadolinium). The figure shows that the field distribution across the gadolinium was not completely uniform. The field varied about 12% from the center to either end of the gadolinium.

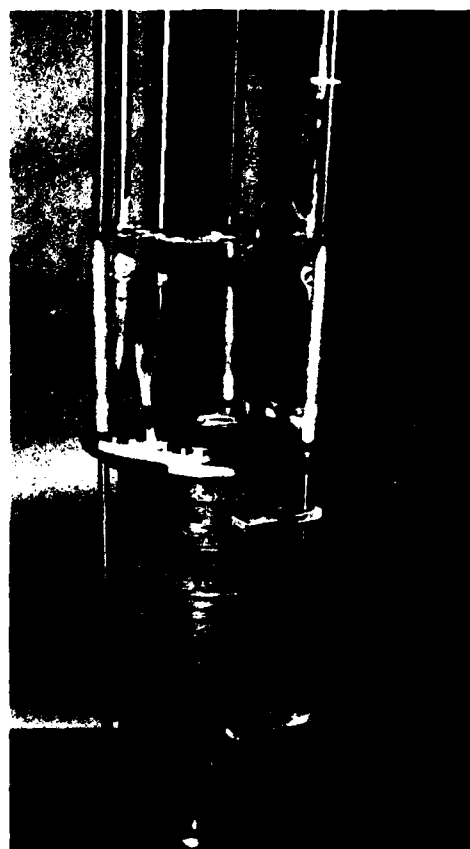


Fig. 10. Superconducting magnet used in the experimental magnetic refrigerator.

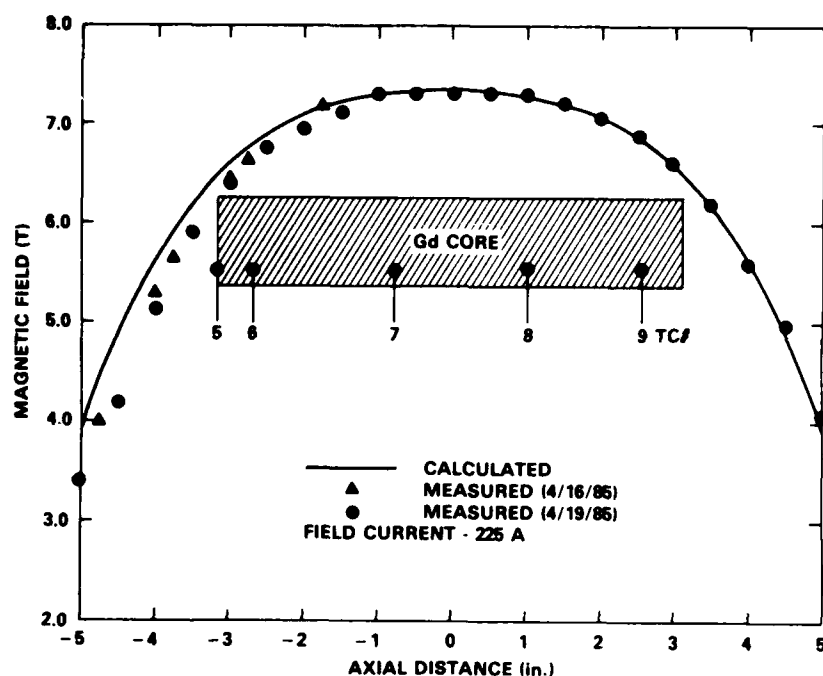


Fig. 11. Magnetic field distribution along the axis of the superconducting magnet. (TC# = Thermocouple number).

Most of the magnetic refrigerator apparatus is shown schematically in Fig. 12. The magnetic material was centered in the magnetic field by placing this apparatus through the warm bore of the magnet's Dewar flask. The passive regenerator and the active ferromagnetic regenerator both were constructed as narrow embossed metal ribbon wound into discrete sections ("pancakes") of material and stacked into a G-10 fiberglass sleeve (see Fig. 13). The passive regenerator was fabricated with copper, the magnetic regenerator with gadolinium. The gadolinium ribbon was embossed using a rolling mill; the process is described in detail by Lare [16]. The formed gadolinium ribbon was sheared into 0.317-cm widths and lengths of it were wound into the pancake sections. The winding mechanism is described by Patton.* These pancakes could then be placed into the fiberglass cylinder as illustrated in Fig. 13.

*Patton, W.G., "Winding Mechanism for Winding Ribbon-Gap Regenerators," Patent Disclosure Application (1985).

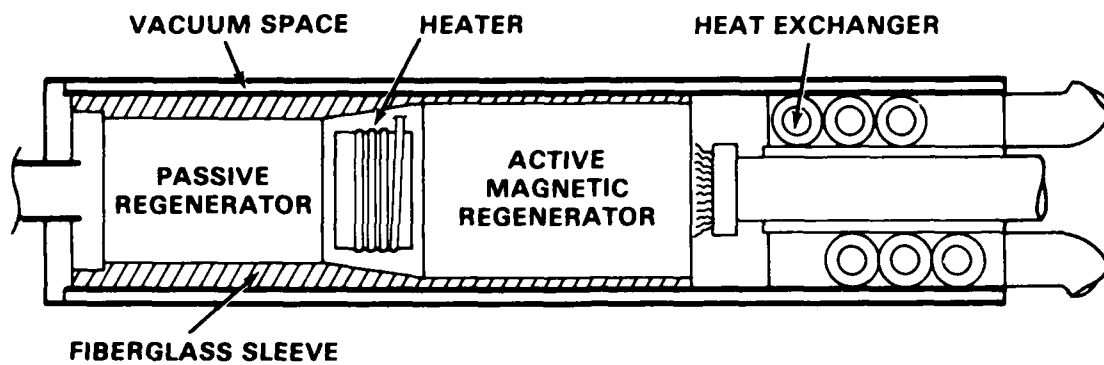


Fig. 12. Magnetic refrigerator apparatus.

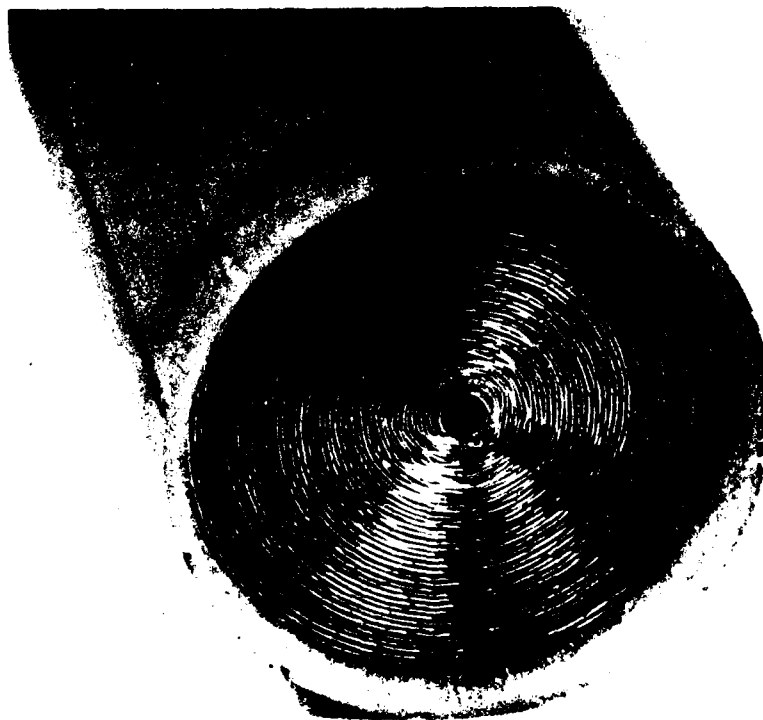


Fig. 13. Gadolinium ribbon regenerator section in the G-10 fiberglass sleeve.

The passive regenerator used a copper wire that also was formed, wound into a pancake, and inserted into a fiberglass cylinder. The embossed bumps on the metal ribbons provided a set of uniformly spaced flow channels separated by a high heat capacity material to provide the regeneration. The copper regenerator had 0.0178-cm embossed bumps on a ribbon 0.0254-cm thick. This provided a packing factor of 65% and a total copper mass of 2.47 kg. The gadolinium, in contrast, had 0.0127-cm embossed bumps on a ribbon 0.0127-cm thick, which produced a packing factor of 50% and a total mass of 0.900 kg.

A finned tube heat exchanger (Fig. 14) was placed at the warm end of the refrigerator to remove the heat of the magnetization process and to maintain a constant temperature at that point. Water flowing through the tube intercepts the heat from the working fluid that passes through the fins of the shell portion of the heat exchanger.

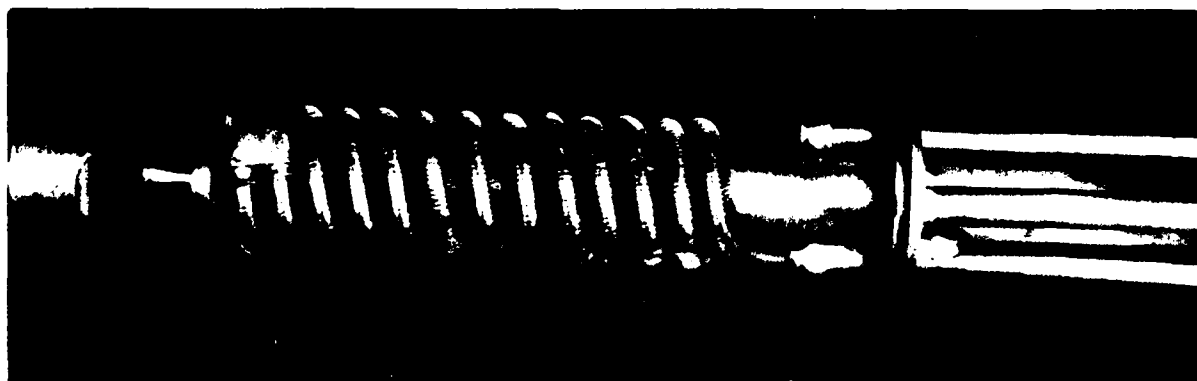


Fig. 14. Finned tube heat exchanger.

In addition, a small heater capable of producing about 20 W of power was placed in the cold section of the apparatus. The heater was shown on Fig. 12. It was intended for use in measuring the refrigerator's performance.

The outlet portion of the finned tube heat exchanger and the copper regenerator were connected to the displacer cylinder on either side of the piston. This displacer was a hydraulic cylinder with a 12.7-cm-diameter piston and a 22.86-cm stroke. Coupled directly to the displacer was a hydraulic cylinder with a 5.08-cm bore and 22.86-cm stroke; this cylinder drove the displacer. A Rexroth hydraulic pump with a four-way proportional valve moved the displacer back and forth under electronic control, thus moving the gaseous working fluid (pressurized N₂ gas) back and forth through the magnetic refrigerator.

Temperatures were measured in the refrigerator components with type T (copper-constantin) thermocouples. These thermocouples were inserted through small holes drilled in the fiberglass tube and into the component material. Number 36 thermocouple wire was used to minimize heat conduction and response time. The thermocouple wire was placed in grooves machined in the outside of the fiberglass tube. Figure 15 shows some of the thermocouples in the magnetic material leading to the right end of the assembly, where they pass through the pressure-tight feed-through. The location of the thermocouples in the magnetic material is shown in Fig. 11, superimposed in relation to the magnetic field. A total of 13 thermocouples were used as follows:

- 3 in the passive regenerator
- 1 on the heater
- 1 in the gas space between the regenerator and the magnetic material
- 7 in the active magnetic regenerator
- 1 in the gas space between the magnetic material and the heat exchanger

The refrigerator was controlled and the data recorded using a small digital laboratory computer equipped with the necessary I/O modules.

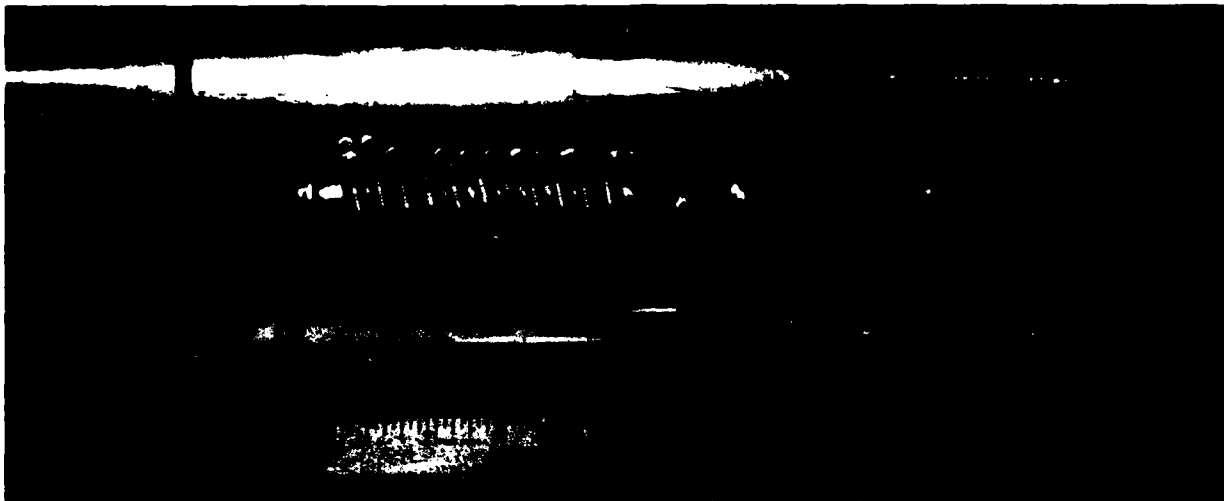


Fig. 15. Magnetic refrigerator assembly.

The magnet current was controlled by the output of a digital-out line which operated the ramp-enable circuit in the magnet exciter. The current level for the magnet was fed back to an analog-in port of the computer using an analogous voltage from the ammeter on the exciter.

The displacer was controlled in a similar manner. The computer program operated through an analog-out line to an electronically controlled hydraulic valve to cause the displacer to go up, stop, or go down. Displacer position was sensed with a linear voltage differential transformer (LVDT) attached to the displacer shaft and fed back to the computer through an analog-in port. Displacer speed was also programmable.

Temperatures, magnet current, displacer position and cycle number were recorded on floppy disks and simultaneously displayed on the computer view terminal. The control and data acquisition program was written in four segments, which corresponded to the four phases of the magnetic cycle. Subroutines were also invoked to display and store the data.

The mass flow of the working fluid, N_2 gas, was varied as a function of temperature to maintain equivalent changes in the heat capacity of the gas and the magnetic material. The mass flow was calculated based on a linear approximation of the adiabatic magnetization process and is plotted in Fig. 16. The mass was varied by assuming the gas pressure would remain the same and the displacer stroke would be varied as a function of gadolinium cold end temperature. This displacer characteristic could then be controlled by the computer program.

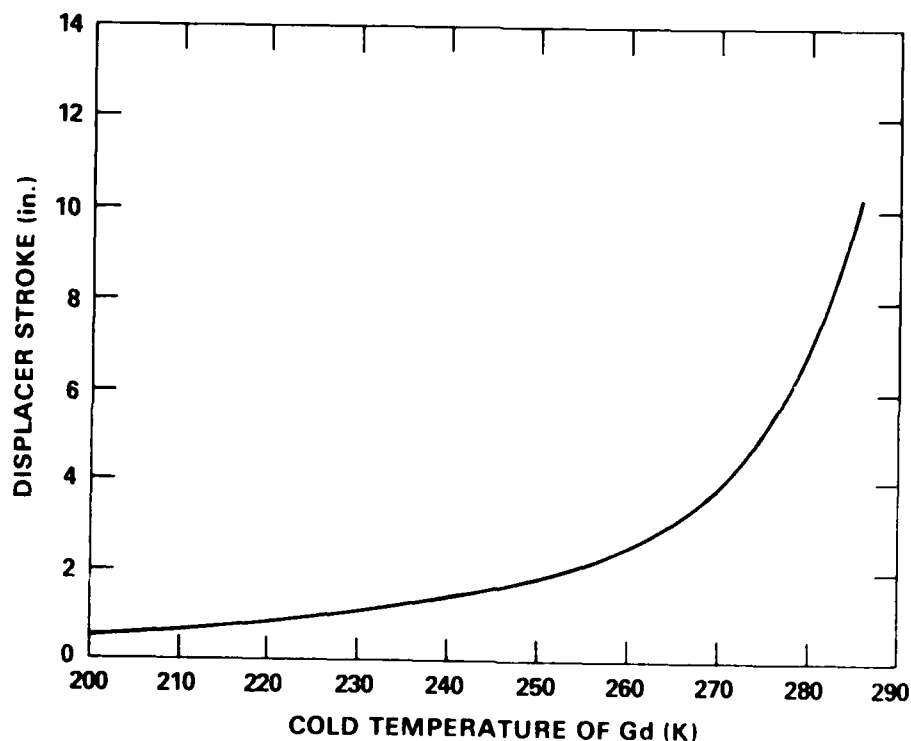


Fig. 16. Calculated mass flow characteristics based on a linear approximation of the adiabatic magnetization process.

The magnet exciter was capable of ramping the magnet up or down from 0 to 220 A in approximately 30 s with an 11-V potential. This magnetization process, plus the displacer movement and the printing of the data, resulted in a 90-s elapsed time span for each cycle of operation. Thus, a 200-cycle cool-down test from room temperature would require approximately 5 h of operation.

After several preliminary experiments to determine the adiabatic temperature change of the material as a function of temperature with a 7-T change in magnetic field, the experimental magnetic refrigerator was used to perform two cool-down experiments starting at room temperature (300 K). One run lasted 8 h, the other 5 h. During each test, the refrigerator was allowed to operate until the supply of liquid helium to cool the superconducting magnet was depleted. Between tests the refrigerator was allowed to warm up throughout, and the displacer was cycled up and down with no magnetic field present to make sure that all parts of the regenerator and active material had reached thermal equilibrium.

After the second test, several problems occurred that prevented any further tests. A leak developed in the heat exchanger, which caused all but two of the thermocouples in the magnetic material to fail; leaking water from the heat exchanger caused movement and created a large pressure drop in the ferromagnetic material. However, a significant amount of data was obtained and is reported.

RESULTS

In the preliminary experiments, the thermocouples implanted in the gadolinium were used to measure the adiabatic magnetization and demagnetization process. Figure 17 compares the measured temperature change resulting from the magnetization step in the gadolinium with previously reported data [9]. Our measurements showed a 25% reduction in the performance of the magnetic material.

The short fall in adiabatic temperature change in this experiment as compared to Benford and Brown's results can be attributed to several factors:

1. About 15% of the difference in adiabatic temperature change can be attributed to the heat capacity of the nitrogen gas surrounding the gadolinium ribbon.
2. There is some heat transfer in the axial direction of the gadolinium material.

3. The G-10 fiberglass tube surrounding the gadolinium has some heat capacity which diminishes the adiabatic temperature rise.
4. The thermocouple preamplifiers used to interface with the computer data acquisition system had at least a 1% order in output.

These four factors also act to reduce the reversibility of the adiabatic temperature change.

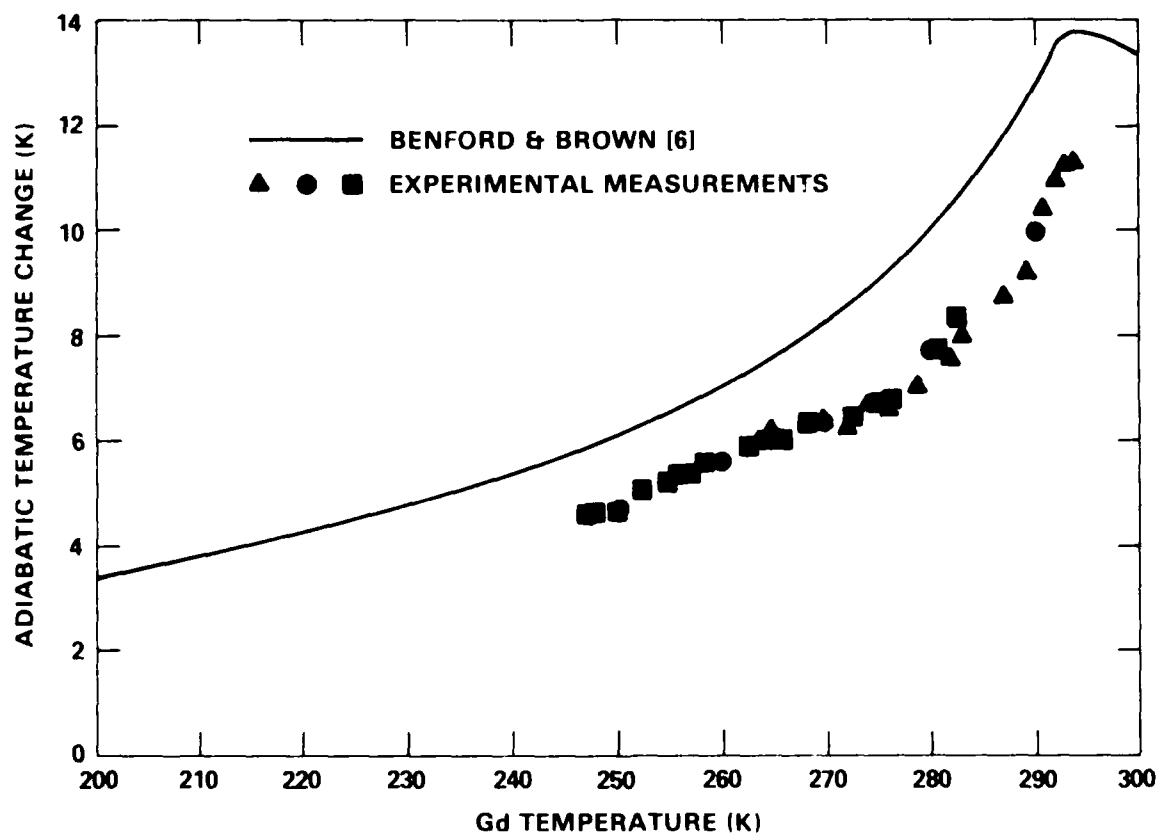


Fig. 17. Measured adiabatic magnetization characteristics for Gd ribbon.

The two cool-down experimental runs conducted with this apparatus were started near room temperature (300 K) and cooled the cold portion of the refrigerator down to a low temperature of 246 K. Cool-down profile of these two runs is shown in Fig. 18. These two cool-down characteristics showed very similar performance; the slight variation resulted from the difference in the mass flow of nitrogen gas for each test. Run 2 was conducted under more nearly optimal mass flow conditions.

In one of the early preliminary runs, before the thermocouples broke, the temperature distribution through the gadolinium was measured. Each set of measurements indicated the temperature profile after each significant event in the cycle. Figure 19 shows these characteristics of the temperature distribution in magnetic material. In addition, the figure also shows the variation of the magnetocaloric effect in the material as a function of temperature and field. This smaller magnetocaloric effect at the lower temperatures could be improved by using other rare-earth metals with decreasing Curie temperatures. This possibility was discussed in the section on the mathematical model (see also Fig. 8).

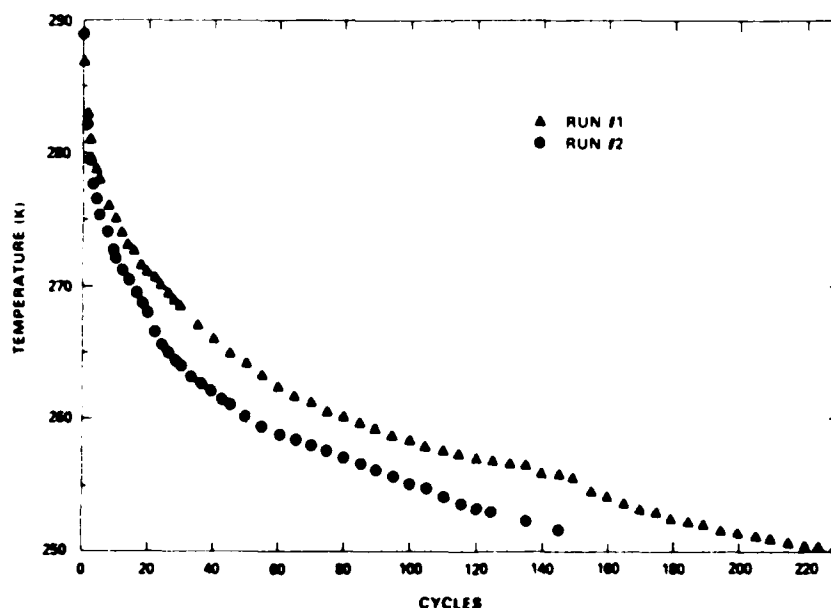


Fig. 18. Measured cool-down profile of the magnetic refrigerator.

The average measured adiabatic temperature change in the magnetic material was about 7°C. The lowest temperature obtained with the experimental apparatus was 246 K, a 50°C temperature difference across the active regenerator. These measurements compare well with the results described earlier on the mathematical model and results described by Brown [5]. Although the math model did not include the passive regenerator in the refrigerator and its associated capacity, the final temperature obtained in the experimental apparatus was close to that calculated in the numerical model.

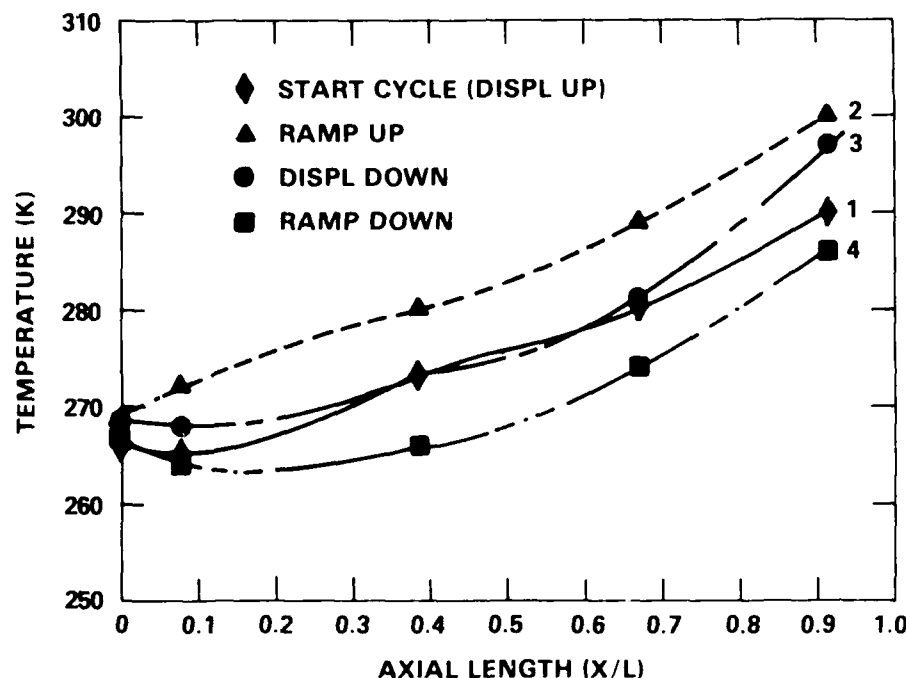


Fig. 19. Measured temperature distribution of the Gd active magnetic regenerator.

CONCLUSIONS

The experimental magnetic refrigerator produced a 50°C temperature span with only a 7°C adiabatic temperature change in the magnetic material. The regeneration process in the magnetic material produced a factor of 7 increase in the temperature span for a single ferromagnetic material. Without a doubt, the active regeneration

concept used in conjunction with the embossed ribbon configuration can successfully produce magnetocaloric refrigeration at temperatures higher than 4 K.

Further, if several rare-earth metals, having significant magnetocaloric effects at decreasing temperatures, were combined as the active magnetic element, the possibility exists for producing a single-stage magnetic refrigerator that could operate over a large temperature span. Such a refrigerator, if developed, offers the possibility of a compact, highly efficient, reliable, shock resistant, closed cycle refrigerator for cooling or liquefying gases from room temperature down to liquid helium temperature (4 K) in only a few stages.

ACKNOWLEDGEMENT

The frequent conversations and advice from Dr. John Barclay of Astronautics, Inc., and efforts of Dr. Sam Brown of DTNSRDC in calculating the magnetic field in the magnetic material using the Classical Molecular Field Theory, as presented in the appendix, and the technical writing assistance of Margaret Knox of DTNSRDC are greatly appreciated.

APPENDIX

CLASSICAL MOLECULAR FIELD THEORY

The strong interaction in a ferromagnetic material that aligns the atomic dipoles in a parallel manner may be represented by some internal field H_M . The thermal agitation of the atoms in the ferromagnetic lattice opposes the orientation of the field. The Curie temperature is defined as the point at which the thermal agitation is of a sufficient magnitude to counteract the spontaneous magnetization.

Weiss [17] developed a phenomenological model for ferromagnetism by assuming that H_M was proportional to the magnetization M (i.e., spontaneous magnetization).

$$H_M = KM \quad (A.1)$$

The symbol K is termed the molecular field constant (or mean field coupling constant). The field H_M is called the molecular field constant. However, the field is sometimes termed the Weiss or exchange field. In the presence of an arbitrary applied field H the actual field acting on a particular dipole H_T is

$$H_T = H + KM \quad (A.2)$$

The demagnetizing and Lorentz (dipole-dipole) fields are ignored because they are small when compared to the molecular field.

SPONTANEOUS MAGNETIZATION REGION

We assume that the atoms of the solid have a total angular momentum quantum number J and have N atoms per unit volume. Then the magnetization of the ferromagnetic material is given, in Gaussian units, by: [18]

$$M = Ng\mu_B J B_J(x) \quad (A.3)$$

$$\text{where } x = \frac{Jg\mu_B H T}{kT} \quad (\text{A.4})$$

$$\text{and } B_J(x) = \left(\frac{2J+1}{2J} \right) \cot h \left[\frac{(2J+1)x}{2J} \right] - \frac{1}{2J} \cot h \left(\frac{x}{2J} \right) \quad (\text{A.5})$$

$$\cot hu = \frac{(e^u - e^{-u})}{(e^u + e^{-u})} \approx u - \frac{u^3}{3} + \frac{2u^5}{15} - \frac{17u^7}{315}$$

The symbols in the above equations have the following meaning. (The numerical values for the atoms are for gadolinium).

k = Boltzmann's constant (1.381×10^{-16} erg/K)

J = total angular momentum

K = mean field coupling constant (calculated)

μ_B = bohr magneton $\frac{\theta h}{2mc} = 0.927 \times 10^{-20}$ erg/gauss

g = Lande factor (dimensionless quantity)

T = temperature in Kelvin

B = magnetic induction (gauss)

H = magnetic field (oersteds)

M = magnetization (magnetic moment/cm³)

N_0 = Avogadro's number = 6.0225×10^{23} mole⁻¹

N = number density of dipoles (0.2596×10^{23} cm⁻³)

T_C = ferromagnetic Curie point

The mean field constant K may be calculated as a function of T_C , the Curie temperature. Above T_C no spontaneous M exists so that Eqs. A.3 and A.4 have only a trivial solution for M .

$$Ng^2\mu_B J (J+1)K = 3kT_C \quad (A.6)$$

Considering the above theory, the equation for the magnetization M of gadolinium may be expressed in detail as

$$M = Ng\mu_B J B_J(x) = \left\{ \left[\frac{2J+1}{2J} \right] \cot h \left[\frac{(2J+1)}{2J} \frac{\mu_B g J (H+KM)}{kT} \right] - \frac{1}{2J} \cot h \left[\frac{\mu_B g J (H+KM)}{2JkT} \right] \right\} Ng\mu_B J \quad (A.7)$$

Dividing through by M the equation is

$$\frac{1}{M} \left\{ \frac{2J+1}{2J} \cot h \left[\frac{(2J+1)}{2J} \frac{\mu_B g J (H+KM)}{kT} \right] - \frac{1}{2J} \cot h \left[\frac{\mu_B g J (H+KM)}{2JkT} \right] \right\} Ng\mu_B J - 1 = 0 \quad (A.8)$$

For a particular field H the magnetization of the gadolinium may be calculated on the computer by a variational procedure which picks an M so that Eq. A.8 equals zero. Once a particular M is determined for a chosen H , B may be determined from the following equation:

$$B = H + 4\pi M \quad (A.9)$$

The permeability of the gadolinium μ is then calculated from

$$\frac{B}{H} = \mu \quad (A.10)$$

REFERENCES

1. Barclay, J.A., "An Analysis of Liquefaction of Helium Using Magnetic Refrigerators," LA-8991, Los Alamos National Laboratory (1981).
2. Lacaze, A.F., B. Beranger, G. Mardion, G. Claudet Bon, "Efficiency Improvements of a Double Acting Reciprocating Magnetic Refrigerator," Cryogenics, Vol. 21, pp. 427 (1983).
3. Stowbridge, T.R., "Cryogenic Refrigerators--an Updated Survey," National Bureau of Standards Report TW-655 (1974).
4. Barclay, J.A., "Magnetic Refrigeration for 4-20 K Applications," AFWAL-TR-83-3120 Report (1983).
5. Brown, G.V., "Magnetic Heat Pumping Near Room Temperature," J. Appl. Phys., Vol. 47 (1976).
6. Barclay, J.A. and W.A. Steyert, "Active Magnetic Regenerator," Patent US-A228836 (1983).
7. Wark, K., Thermodynamics, McGraw-Hill (1966) Chap. 13.8, pp. 399-402 (1966).
8. Green, G.F., W.G. Patton, and J. Stevens, "Low Temperature Ribbon Regenerator," 4th International Cryocooler Conference (1985).
9. Benford, S.M. and G.V. Brown, "T-S Diagram for Gadolinium Near the Curie Temperature," J. Appl. Phys., Vol. 52 (1981).
10. "Numerical Solution of the Poisson Equation in a Non-Uniform Triangle Mesh (TRIM), A.M. Winslow UCRL-7788-T (1965).
11. Hurwitz, M.M., "Additions to the NASTRAN User's Manual and Theoretical Manual for a Thermostructural Capability for NASTRAN Using Isoparametric Finite Elements," DTNSRDC Report CMC-1-73 (Jan 1973).
12. Griffel, M., R.E. Skochdopole, R.E., and F.H. Spedding, "The Heat Capacity of Gadolinium from 15 to 355 K," Physical Review, Vol. 93, No. 4 (1954).

13. Kays and London, "Compact Heat Exchangers," 2nd Edition (1964).
14. Schroeder, E.A., "Transient Analysis of a Magnetic Refrigerator," DTNSRDC Report 85/099 (1985)
15. Benford, S.M., "The Magnetocaloric Effect in Dysprosium," J. Appl. Phys., Vol. 50 (1979).
16. Lare, P.J., "Forming of Uniform Channels on a Gadolinium Ribbon," Artech Corporation Report J8350.10-FR (1983).
17. Kittel, Charles, "Introduction to Solid State Physics," John Wiley & Sons, New York, 3rd Edition (1968).
18. Brown, Gerald V., "Magnetic Stirling Cycles--A New Application for Magnetic Materials, IEEE Trans Magne. Vol. MAG-13, No. 5 (Sept 1977).

INITIAL DISTRIBUTION

Copies

	Copies	Code
1 CONR/Arlington (414, Edlesack)		
1 AFWAL/FIEE	2	012.3, Moran
Wright-Patterson Air Force Base		
Dayton, OH 45433	1	27
Attn: Paul Lindquist	2	271, Stevens
1 Chemical Engineering Science Division		
Code 773.3	1	2712, Superczynski
NBS-325 Broadway		
Boulder, CO 80303	20	2712, Green
Attn: Dr. Ray Wadebaugh	1	5211, Knox
12 DTIC	10	5211.1, Rept Control
	1	522.1, TIC Carderock
	1	522.2, TIC Annapolis
	1	5231, Office Services

DTNSRDC ISSUES THREE TYPES OF REPORTS:

1. **DTNSRDC reports, a formal series**, contain information of permanent technical value. They carry a consecutive numerical identification regardless of their classification or the originating department.
2. **Departmental reports, a semiformal series**, contain information of a preliminary, temporary, or proprietary nature or of limited interest or significance. They carry a departmental alphanumerical identification.
3. **Technical memoranda, an informal series**, contain technical documentation of limited use and interest. They are primarily working papers intended for internal use. They carry an identifying number which indicates their type and the numerical code of the originating department. Any distribution outside DTNSRDC must be approved by the head of the originating department on a case-by-case basis.

END

11-87

DTIC